



Increased Autophagy during Smooth Muscle Cell Differentiation from Human Adipose-Derived Stem Cells

Shing-Hwa Lu^{1,2}, Alex T.L. Lin^{2,1}, An-Hsiang Chang³

^{1,2,3} Department of Urology, Taipei Veterans General Hospital, Taipei, Taiwan

^{1,2} Department of Urology, School of Medicine, National Yang-Ming University, Taipei, Taiwan

***Corresponding Author: Dr. Shing-Hwa Lu,**

Department of Urology, Taipei Veterans General Hospital, No 201, Sec 2, Shih-Pai Road, Taipei City 11211, Taiwan, ROC. , Fax: 886-2-28757540

ABSTRACT

Background

To evaluate the role of autophagy and the molecular changes in the process of smooth muscle cells (SMCs) differentiation from human adipose-derived stem cells (hADSCs) and establish a protocol for inducing this differentiation.

Methods

The differentiation of hADSCs into SMCs was induced using the smooth muscle induction medium (SMIM) with a low serum level. Real-time PCR was used to examine the mRNA expression of smooth muscle marker genes. In addition, we used Western blot analysis and immuno fluorescence staining to evaluate changes in the protein level.

Results

We observed an increase in the expression of smooth muscle marker genes, alpha-smooth muscle actin (α -SMA) and myosin heavy chain (MHC), in hADSCs exposed to SMIM for 6 weeks. The cellular complexity and granularity were increased in induced hADSCs, suggesting an increase in the content of intracellular organelles during the SMC differentiation process. The content of lysosomes, but not of mitochondria or endoplasmic reticulum, was significantly increased. The increased protein content of the lysosomal-associated membrane protein 1 confirmed the increase in the lysosomal content during SMC differentiation. By contrast, the conversion from LC3-I to LC3-II was increased during SMC differentiation, with a significant increase after 3 weeks of differentiation.

Conclusions

These results suggest that autophagy is significantly upregulated in the early stage of SMC differentiation. Autophagy might play a crucial role in SMC differentiation from hADSCs. Human ADSCs may be a potential biomaterial for urinary incontinence treatment and bladder reconstitution.

Keywords: human adipose-derived stem cells; differentiation; smooth muscle cell; autophagy

1. INTRODUCTION

Autophagy is the process needed to eliminate unwanted cytoplasmic materials in order to

prevent cellular damage. There were accumulating evidence suggesting that autophagy plays a critical role in the homeostatic control of the function of stem cell function during tissue



regeneration, aging, and cellular reprogramming (20).

The origin of smooth muscle cells (SMCs) during both development and adult life is heterogeneous. Their progenitors mainly arise from the splanchnic mesoderm and the neural crest during development (16). In addition, they are found in circulating blood (25). In postnatal life, SMCs progenitors arise from the bone marrow (6). Some studies have reported that smooth muscle-like cells can be derived from bone marrow cells both *in vitro* (6, 29) and *in vivo* (18, 21). The bone marrow is the major source of two types of stem cell, hematopoietic and nonhematopoietic mesenchymal stem cells, in postnatal life. Furthermore, both the bone marrow and adipose-derived stem cells (ADSCs) have self-renewal capacity and long-term viability, and can potentially differentiate into diverse cell types such as adipogenic, osteogenic, chondrogenic, myogenic, neurogenic, and cardiomyogenic lineages when treated with specialized induction mediums (33). ADSCs can be obtained from the abundant adipose tissue through a minimally invasive procedure, and ADSCs can be an ideal source of autologous stem cells for tissue engineering and in regenerative medicine (2, 28).

Mature SMCs can undergo reversible changes in their phenotype in response to changes in the local environment (16). Some soluble factors such as TGF- β 1, platelet-derived growth factor, retinoic acid, interleukin-1, L-ascorbic acid, sphingosylphosphorylcholine, and thromboxane A2 regulate the differentiation of SMCs (1, 31). In addition, studies have indicated that SMCs express the contractile differentiated phenotype when they are not in the proliferative state. In this study, we used the smooth muscle induction medium (SMIM) with a low serum level and containing heparin, which induces alpha-SMA expression (3), in combination with the

MCDB131 medium supplemented with 1% FBS as the differentiation condition medium for inducing the differentiation of human ADSCs (hADSCs) into SMCs (22). Several *in vitro* models are available for studying SMC differentiation. However, unlike other cell lineage differentiation, SMC differentiation is not terminal and can be completely reversed under some stimuli; their underlying mechanisms are more complicated. Accumulating evidence has revealed that numerous signal pathways and molecules, such as collagen IV, integrins, SRF-myocardin complex, Nox4/H₂O₂, HDAC7, and microRNAs, play a major role in SMC differentiation.(30) However, the mechanism underlying the differentiation of stem cells into SMCs is not fully understood. This study was conducted to realize the molecular changes during SMC differentiation from hADSCs.

2. MATERIALS AND METHODS

Cells and culture. This study was granted approval in National Yang-Ming University in Taipei with the IRB number: 990023. The hADSCs were obtained from Invitrogen: STEMPRO Human Adipose-Derived Stem Cells (R7788-115) expressing a flow cytometry cell-surface protein profile positive for CD29, CD44, CD73, CD90, CD105, and CD166 (>95%) and negative for CD14, CD31, CD45, and Lin1 (<2%). The cells were maintained in MesenPRO RSTM medium (Invitrogen) containing 1% L-glutamax (Invitrogen) and 1% penicillin/streptomycin (Invitrogen) and incubated at 37 °C in 5% CO₂. The cells were expanded at a density of 5000 cells/cm² until they reached 90% confluency. The medium was replaced every 3-4 days. All the cells used in the experiments were passaged for 5-10 generations.



SMC differentiation. The expanded cells of hADSCs were seeded at a density of 5000 cells/cm² in complete MesenPRO RSTM medium until they reached 70%-80% confluency to induce SMC differentiation in SMIM. SMIM consists of MCDB131 (Gibco) with 1% FBS (Gibco), 1% penicillin/streptomycin (Gibco), and 100 units/mL of heparin (Sigma). The medium was replaced every 3–4 days.

Quantitative real-time PCR. The expression of alpha-smooth muscle actin (α -SMA), SM22 α , calponin, caldesmon, and myosin heavy chain (MHC) was quantified in induced hADSCs (primers used are listed in Table 1). Total RNA was extracted using the total RNA miniprep kit (Axygen). Each RNA sample (5 μ g) was subjected to cDNA synthesis by using YouPrime Ready-to-Go cDNA beads (Amersham Pharmacia Biotech) combined with a random primer. All samples were treated using the RNase-free DNase set (Qiagen). Quantitative real-time PCR was performed in an ABI Prism 7700 (PE Applied Biosystems). Each cDNA was analyzed in triplicates by using the QuantiTect SYBR Green PCR Kit (Qiagen). The relative abundance of transcripts was normalized to the constitutive expression of β -actin.

Western blot analysis. The hADSC induced to differentiate into the SMC lineage after a period of 3-6 weeks in SMIM medium, will be washed with cold PBS, and the cell lysate was prepared using RIPA buffer (150 mM NaCl, 50 mM Tris-HCl, 0.1% SDS, 0.5% sodium deoxycholate, and 0.1% Triton X-100) plus 10 μ g/mL aprotinin (Sigma), 2 mM EGTA (Sigma), 2 mM Na₃VO₄ (Sigma), and 1 mM PMSF (Sigma). Furthermore, 30 μ g of protein was separated through SDS-PAGE and transferred onto polyvinylidene fluoride (PVDF) membranes (PALL Life Science). Unspecific binding sites on PVDF

membranes were blocked, and the membrane was hybridized with primary antibodies, anti-MHC (Millipore), anti-SMA (Millipore), LC3B (Cell Signaling Technology), lysosomal-associated membrane protein 1 (LAMP-1, Cell Signaling Technology), and anti- β -actin (Santa Cruz Biotech), following incubation with horseradish peroxidase (HRP)-conjugated secondary antibodies. The membranes were then developed using Immobilon Western chemiluminescent HRP substrates (Millipore). Images were captured using the Luminescence/Fluorescence Imaging System (GE Healthcare), and signal intensity was quantified using the Multi-Gauge image analysis software (FUJIFILM).

Immunofluorescence studies. Glass coverslips were placed at the bottom of the 6 well plate before coculturing. When the induction of differentiation reached 60%-70% confluence, the culture medium was removed and the wells were washed twice with PBS. Fixation was performed by adding 100 μ L of 3.7% paraformaldehyde (Sigma) per well, followed by washing three times with PBS. For permeabilization, 100 μ L of 1% Triton/PBS was added, followed by 0.02% Tween 20/PBS. Furthermore, 100 μ L of PBS containing a primary antibody (1:100) was added, and the plate was placed in a 37 °C water bath for 45 min. The plate was washed three times with 0.02% Tween 20/PBS. Furthermore, 100 μ L of PBS containing a secondary antibody at a ratio of 1:50 was added in each well, and the plate was placed in a 37 °C water bath for 45 min. The antibodies of phalloidin and α -SMA were purchased from Millipore. When the reaction time was over, the plate was washed three times with 0.02% Tween 20/PBS for 5 min and then washed with PBS for 5 min. The coverslips were dried at 37 °C for 45 min in the dark. Before analysis under a microscope, 10-15 μ L of Dabco mounting media



(PBS, 50%-60% glycerol, and 2.5% 1, 4 diazobicyclo (2, 2, 2)- octane) was added, and coverslips were sealed using a transparent nail polish. The coverslips were observed under a fluorescent microscope, and the wavelengths for example FITC excitation and emission were set at 488 and 515 nm, respectively.

Images were captured through the Leica TCS SP2 CLSM analysis.

Determination of lysosomal, mitochondrial, and endoplasmic reticulum contents.

The fluorescent dye LysoTracker green (Molecular Probes), which specifically binds to acidic lysosomes, was used to examine the lysosomal content. The fluorescent dye MitoTracker green (Molecular Probes), which appears to localize in the mitochondria regardless of the mitochondrial membrane potential, was used to evaluate the mitochondrial content. The fluorescent dye ER Tracker Green (Molecular Probes), which is a cell-permeant, live-cell stain and highly selective for the endoplasmic reticulum (ER), was used to examine the ER content. The cells were trypsinized and resuspended in 0.5 mL of PBS buffer containing 50 μ M LysoTracker Green, 50 nM MitoTracker Green, and 1 μ M ER Tracker Green. After incubation for 10 min at 25 $^{\circ}$ C in the dark, the cells were immediately transferred into a tube on ice for the flow cytometry analysis.

Statistical Analyses. Statistical analyses were performed through the Student *t* test.

A probability value of <0.05 was considered statistically significant.

3. RESULTS

Cell morphology image. This study use of SMIM with a low serum level induced the

differentiation of hADSCs into SMCs. During this differentiation, the cell morphology of hADSCs changed: they became spindle shaped with a typical hills- and-valleys morphology as observed in SMCs both at 3 and 6 weeks (Fig. 1).

Real-time PCR analysis. After 3 weeks of SMC differentiation from hADSCs, the mRNA expression levels of SMC markers, namely α -SMA, SM22 α , calponin, caldesmon, and MHC, increased (Fig. 2).

Western blot analysis. The results of the Western blot analysis were similar to those of real-time PCR. The protein expression of MHC and α -SMA was markedly increased during SMC differentiation from hADSCs both at 3 and 6 weeks (Fig. 3).

Immunofluorescence staining images. The immunofluorescence staining of the cellular actin cytoskeleton in hADSCs after SMC differentiation revealed a high ratio of α -SMA within stress fibers (F-actin)(Fig. 4).

Flow cytometry analysis. The forward scatter (FSC, Fig. 5A) and side scatter (SSC, Fig. 5B) parameters exhibited an increase in SMC that differentiated from hADSCs, suggesting an increase in the intracellular complexity, granularity, and cell volume. We examined the content of intracellular organelles including lysosomes, mitochondria, and ER and observed a significant increase in the intracellular content of lysosomes but not in that of mitochondria and ER (Fig. 5C).

Western blot analysis for lysosomal-associated membrane protein. The increased protein content of LAMP-1 confirmed the increase in the lysosomal content during SMC differentiation (Fig. 6). By contrast, the conversion from LC3-I to LC3-II increased during SMC differentiation, and a significant increase was observed at 3



weeks after differentiation (Fig. 6). These results suggest that autophagy is upregulated in the early stage of SMC differentiation.

4. DISCUSSION

Abnormal SMC differentiation plays critical roles in the pathogenesis and progression of several diseases including atherosclerosis. Moreover, SMC differentiation from stem cells is potentially useful in cell-based therapies in regenerative medicine. Therefore, understanding factors that mediate the process and regulation of SMC differentiation is crucial. We have demonstrated that muscle-derived cells (MDCs) isolated from the rat skeletal muscle can form myotubes and incorporate them into the small intestinal submucosa, thus producing contractile biomaterials with a performance suitable for urological regeneration. Furthermore, human muscle-derived cells (hMDCs) have been successfully isolated, characterized, and purified from human skeletal muscle. and found that multipotent differentiation of hMDCs into several cell lineages including adipose, osteogenic, chondrogenic, and myogenic cell lineages is feasible (10, 12-15). We also clarified the smooth muscle differentiation capability of purified hMDCs that were isolated from the human skeletal muscle (11). However, because of the low proliferative capability of hMDCs in culture, other cell sources should be explored. In this study, the hADSCs from Invitrogen were selected to succeed hMDCs, and SMC differentiation from hADSCs was successfully achieved using SMIM with a low serum level. However, additional studies should confirm the differentiation condition of hADSCs before they are used in subsequent studies.

Although SMCs exhibit morphological and physiological heterogeneity, they have some common features such as the spindle shape, low

proliferative rate, decreased extracellular matrix synthesis, ligand-induced contractility, and cytoskeletal and contractile protein diverse expression. These contractile proteins include α -SMA (26), calponin (27), SM22 α (9), caldesmon (5), and MHC (4). SMC differentiated from hADSCs exhibit a spindle shape with a typical hills-and-valleys morphology (Fig. 1).

The results of real-time PCR revealed that the expression of early smooth muscle genes, α -SMA and calponin, and late smooth muscle genes, SM22 α , caldesmon, and MHC, was upregulated in induced hADSCs (Fig. 2). Western blot analysis confirmed the real-time PCR results with a significant increase in the expression of SMC specific genes, α -SMA and MHC, at the protein level; a stable increased expression was observed after 3 and 6 weeks of differentiation (Fig. 3). In addition, immunofluorescence staining of the cellular actin cytoskeleton in induced hADSCs revealed a high ratio of α -SMA within stress fibers (Fig. 4). These results indicated that SMC differentiation from hADSCs can be successfully induced using SMIM with a low serum level.

During SMC differentiation from hADSCs, we examined the increase in the cellular complexity and granularity in induced hADSCs (Fig. 5), suggesting an increase in the content of intracellular organelles. We observed that the intracellular content of lysosomes, but not of mitochondria and ER, was significantly increased (Fig. 5). The increased protein content of LAMP-1 confirmed the increase in the lysosomal content during SMC differentiation (Fig. 6). By contrast, the conversion from LC3-I to LC3-II was increased during SMC differentiation, with a significant increase at 3 weeks (Fig. 6). These results suggest that autophagy is upregulated in the early stage of SMC differentiation. Autophagy is crucial for stem cell differentiation because it may provide bioenergetic support for



differentiation (17, 19, 23) and it can be a crucial therapeutic target for improving transplant outcomes (8). The result of our study indicated that the upregulation of autophagy in the early stage of SMC differentiation might recommend the need of more bioenergetic support in that stage.

Kuismanen et al. (7) first described the treatment of autologous ADSCs in combination with collagen gel for five female patients with SUI in a pilot study. The mixture of ADSCs and collagen gel was injected transurethrally into the urethral sphincters through a urethrocystoscope. Three out of five patients displayed a negative cough test with full bladder filled with 500 mL of saline and 2 out of 5 patients experienced improvement of symptoms in 12-month follow-up. Zhao et al. (32) used a combination of autologous ADSCs and controlled-release nerve growth factor for the treatment of SUI rat by periurethral injection. This treatment enhanced urethral muscle layer distribution, increased the neuronal density of urethra, improved abdominal leak point pressure, and reduced urethral perfusion pressure in SUI rats. Most recently, Silwal Gautam et al. (24) reported that autologous ADSCs injected into cryo-injured rabbit urethras could reconstruct skeletal and smooth muscle areas in the cell-implanted regions. Compared to the cell-free control group, leak point pressure of the cell-implanted group was significantly higher at 14 days after implantation. Therefore, injection of ADSCs into the urethra has the potential for tissue regeneration and could be used for the management of urinary incontinence.

ADSCs might be a potential biomaterial for urinary incontinence treatment and bladder reconstitution.

In summary, we observed that autophagy is upregulated in the early stage of SMC differentiation from hADSCs. However, the role

of autophagy in SMC differentiation from hADSCs remains unclear. Further research should be directed toward improving the differentiation efficiency and growth stability of these SMCs. Additional functional property studies on SMCs that are differentiated from hADSCs are required to enable their use in urological regeneration.

ACKNOWLEDGEMENTS

The authors would like to thank for the support of the research grant from the Ministry of Science and Technology, Republic of China, grant No. NSC 99-2314-B-010-003-MY3.

REFERENCES

1. Arakawa E, Hasegawa K, Irie J, Ide S, Ushiki J, Yamaguchi K, Oda S, and Matsuda Y. L-Ascorbic Acid Stimulates Expression of Smooth Muscle-Specific Markers in Smooth Muscle Cells both In Vitro and In Vivo. *Journal of Cardiovascular Pharmacology* 42: 745-751, 2003.
2. Dai R, Wang Z, Samanipour R, Koo K-i, and Kim K. Adipose-Derived Stem Cells for Tissue Engineering and Regenerative Medicine Applications. *Stem Cells Int* 2016: 19, 2016.
3. Desmouliere A, Rubbia-Brandt L, Grau G, and Gabbiani G. Heparin induces alpha-smooth muscle actin expression in cultured fibroblasts and in granulation tissue myofibroblasts. *Lab Invest* 67: 716-726, 1992.
4. Frid MG, Printesva OY, Chiavegato A, Faggini E, Scatena M, Koteliansky VE, Pauletto P, Glukhova MA, and Sartore S. Myosin heavy-chain isoform composition and distribution in developing and adult



- human aortic smooth muscle. *J Vasc Res* 30: 279-292, 1993.
5. Frid MG, Shekhonin BV, Koteliansky VE, and Glukhova MA. Phenotypic changes of human smooth muscle cells during development: late expression of heavy caldesmon and calponin. *Dev Biol* 153: 185-193, 1992.
 6. Kashiwakura Y, Katoh Y, Tamayose K, Konishi H, Takaya N, Yuhara S, Yamada M, Sugimoto K, and Daida H. Isolation of bone marrow stromal cell- derived smooth muscle cells by a human SM22alpha promoter: in vitro differentiation of putative smooth muscle progenitor cells of bone marrow. *Circulation* 107: 2078-2081, 2003.
 7. Kuismanen K, Sartoneva R, Haimi S, Mannerström B, Tomás E, Miettinen S, and Nieminen K. Autologous Adipose Stem Cells in Treatment of Female Stress Urinary Incontinence: Results of a Pilot Study. *Stem Cells Translational Medicine* 3: 936-941, 2014.
 8. Leveque L, Le Texier L, Lineburg KE, Hill GR, and MacDonald KP. Autophagy and haematopoietic stem cell transplantation. *Immunol Cell Biol* 93: 43-50, 2015.
 9. Li L, Miano JM, Cserjesi P, and Olson EN. SM22 alpha, a marker of adult smooth muscle, is expressed in multiple myogenic lineages during embryogenesis. *Circ Res* 78: 188-195, 1996.
 10. Lu SH, Cannon TW, Chermanski C, Pruchnic R, Somogyi G, Sacks M, de Groat WC, Huard J, and Chancellor MB. Muscle-derived stem cells seeded into acellular scaffolds develop calcium-dependent contractile activity that is modulated by nicotinic receptors. *Urology* 61: 1285-1291, 2003.
 11. Lu SH, Lin AT, Chen KK, Chiang HS, and Chang LS. Characterization of smooth muscle differentiation of purified human skeletal muscle-derived cells. *J Cell Mol Med* 15: 587-592, 2011.
 12. Lu SH, Sacks MS, Chung SY, Gloeckner DC, Pruchnic R, Huard J, de Groat WC, and Chancellor MB. Biaxial mechanical properties of muscle-derived cell seeded small intestinal submucosa for bladder wall reconstitution. *Biomaterials* 26: 443-449, 2005.
 13. Lu SH, Wei CF, Yang AH, Chancellor MB, Wang LS, and Chen KK. Isolation and characterization of human muscle-derived cells. *Urology* 74: 440-445, 2009.
 14. Lu SH, Yang AH, Chen KK, Chiang HS, and Chang LS. Purification of human muscle-derived cells using an immunoselective method for potential use in urological regeneration. *BJU Int* 105: 1598-1603, 2010.
 15. Lu SH, Yang AH, Wei CF, Chiang HS, and Chancellor MB. Multi-potent differentiation of human purified muscle-derived cells: potential for tissue regeneration. *BJU Int* 105: 1174-1180, 2010.
 16. Miano JM. Mammalian smooth muscle differentiation: origins, markers and transcriptional control. *Results and Problems in Cell Differentiation* 38: 39-59, 2002.
 17. Mizushima N, and Levine B. Autophagy in mammalian development and differentiation. *Nat Cell Biol* 12: 823-830, 2010.
 18. Orlic D, Kajstura J, Chimenti S, Bodine DM, Leri A, and Anversa P. Bone marrow stem cells regenerate infarcted



- myocardium. *Pediatr Transplant* 3: 86-88, 2003.
19. Ozeki N, Mogi M, Hase N, Hiyama T, Yamaguchi H, Kawai R, Kondo A, Matsumoto T, and Nakata K. Autophagy-related gene 5 and Wnt5 signaling pathway requires differentiation of embryonic stem cells into odontoblast-like cells. *Exp Cell Res* 341: 92-104, 2016.
20. Pan H, Cai N, Li M, Liu GH, and Izipisua Belmonte JC. Autophagic control of cell 'stemness'. *EMBO Molecular Medicine* 5: 327-331, 2013.
21. Religa P, Bojakowski K, Maksymowicz M, Bojakowska M, Sirsjo A, Gaciong Z Fau - Olszewski W, Olszewski W Fau - Hedin U, Hedin U Fau - Thyberg J, and Thyberg J. Smooth-muscle progenitor cells of bone marrow origin contribute to the development of neointimal thickenings in rat aortic allografts and injured rat carotid arteries. *Transplantation* 74: 1310-1315., 2002.
22. Rodriguez LV, Alfonso Z, Zhang R, Leung J, Wu B, and Ignarro LJ. Clonogenic multipotent stem cells in human adipose tissue differentiate into functional smooth muscle cells. *Proc Natl Acad Sci U S A* 103: 12167-12172, 2006.
23. Salemi S, Yousefi S, Constantinescu MA, Fey MF, and Simon HU. Autophagy is required for self-renewal and differentiation of adult human stem cells. *Cell Res* 22: 432-435, 2012.
24. Silwal Gautam S, Imamura T, Ishizuka O, Lei Z, Yamagishi T, Yokoyama H, Minagawa T, Ogawa T, Kurizaki Y, Kato H, and Nishizawa O. Implantation of Autologous Adipose-Derived Cells Reconstructs Functional Urethral Sphincters in Rabbit Cryoinjured Urethra. *Tissue Engineering Part A* 20: 1971-1979, 2014.
25. Simper D, Stalboerger PG, Panetta CJ, Wang S, and Caplice NM. Smooth muscle progenitor cells in human blood. *Circulation* 106: 1199-1204, 2002.
26. Skalli O, Pelte MF, Pecelet MC, Gabbiani G, Gugliotta P, Bussolati G, Ravazzola M, and Orci L. Alpha-smooth muscle actin, a differentiation marker of smooth muscle cells, is present in microfilamentous bundles of pericytes. *J Histochem Cytochem* 37: 315-321, 1989.
27. Small JV, and Gimona M. The cytoskeleton of the vertebrate smooth muscle cell. *Acta Physiol Scand* 164: 341-348, 1998.
28. Tsuji W, Rubin JP, and Marra KG. Adipose-derived stem cells: Implications in tissue regeneration. *World Journal of Stem Cells* 6: 312-321, 2014.
29. Wolf NS, Penn PE, Rao D, and McKee MD. Intraclonal plasticity for bone, smooth muscle, and adipocyte lineages in bone marrow stroma fibroblastoid cells. *Exp Cell Res* 290: 346-357, 2003.
30. Xie CQ, Ritchie RP, Huang H, Zhang J, and Chen YE. Smooth muscle cell differentiation in vitro: Models and underlying molecular mechanisms. *Arteriosclerosis, thrombosis, and vascular biology* 31: 1485-1494, 2011.
31. Yun DH, Song HY, Lee MJ, Kim MR, Kim MY, Lee JS, and Kim JH. Thromboxane A(2) modulates migration, proliferation, and differentiation of adipose tissue-derived mesenchymal stem cells. *Experimental & Molecular Medicine* 41: 17-24, 2009.
32. Zhuang WZ, Long LM, Ji WJ, and Liang ZQ. Rapamycin induces differentiation of

glioma stem/progenitor cells by activating autophagy. *Chin J Cancer* 30: 712-720, 2011.

33. Zuk PA, Zhu M, Mizuno H, Huang J, Futrell JW, Katz AJ, Benhaim P, Lorenz HP, and Hedrick MH. Multilineage cells

from human adipose tissue: implications for cell-based therapies. *Tissue Eng* 7: 211-228, 2001



Figure 1. Cell morphology changes ($\times 40$ magnification) in hADSCs during SMC differentiation from hADSCs. The typical hills-and-valleys morphology was noted at 3 weeks and 6 weeks differentiation.

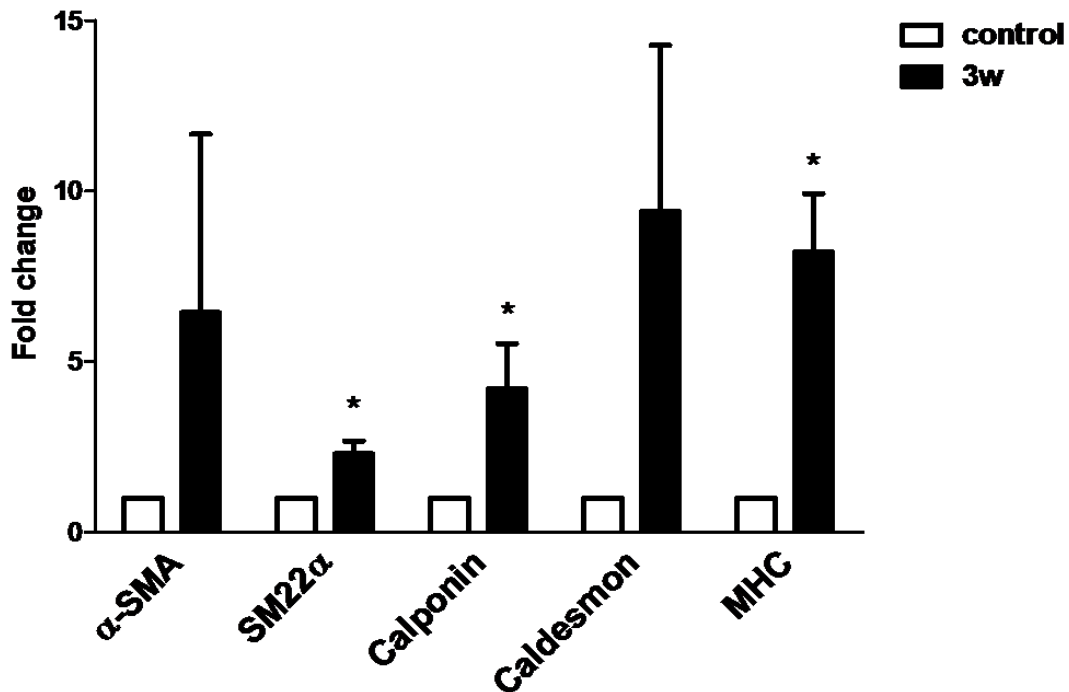


Figure 2. Increase in the mRNA expression of SMC markers during SMC differentiation from hADSCs. The mRNA expression of SMC markers, such as α -SMA, SM22 α , calponin, caldesmon, and MHC, were determined through real-time PCR. β -actin was used as an internal control. Data were represented as mean \pm SEM from at least three independent experiments with duplicate and statistical analysis was performed through a paired t test (* $P < 0.05$).

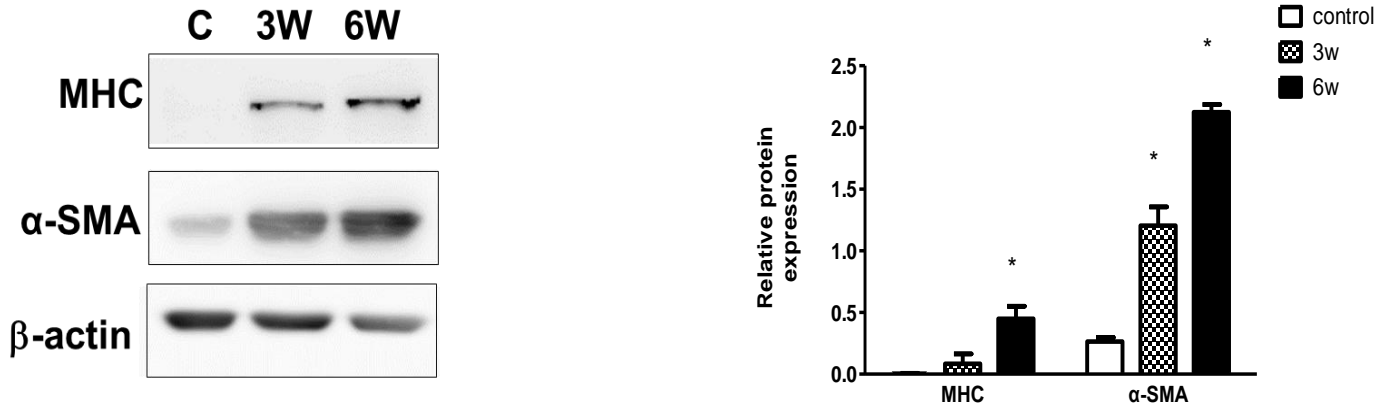


Figure 3. Increased protein expression of SMC markers during SMC differentiation from hADSCs. The MHC and α -SMA proteins were detected through the Western blot analysis. β -actin was used as an internal control. Data were represented as mean \pm SEM from at least three independent experiments with duplicate, and statistical analysis was performed through a paired t test ($*P < 0.05$).

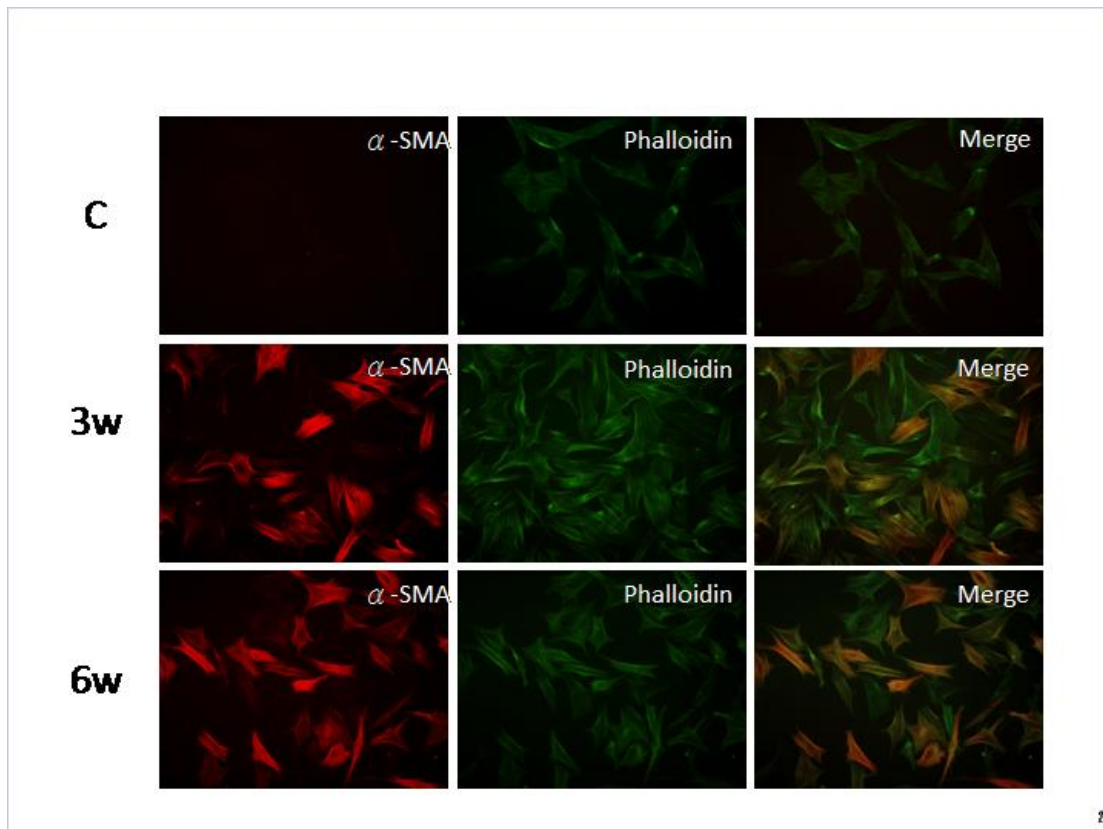


Figure 4. Alteration in the cellular actin cytoskeleton ($\times 100$ magnification) of hADSCs during SMC differentiation. The colocalization of stress fibers (F-actin) with α -SMA indicated the synthesis of α -SMA during SMC differentiation, and a high ratio of α -SMA was observed within stress fibers. Phalloidin (green) was used to stain stress fibers (F-actin), and α -SMA-TRITC (red) was used to stain α -SMA.

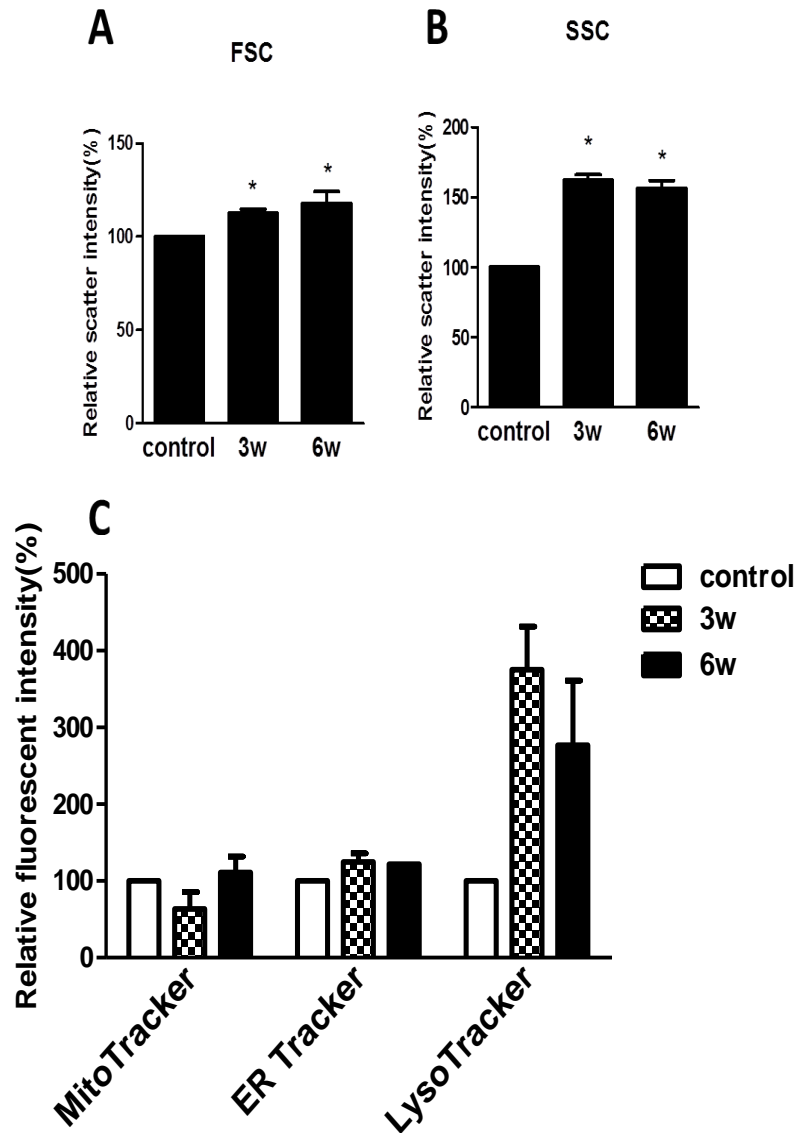


Figure 5. Increased side-scatter intensity and lysosomal content during SMC differentiation from hADSCs. (A, B) Increased cellular complexity and granularity during SMC differentiation from hADSCs. The FSC (A) and SSC (B) parameters were detected through flow cytometry. Data were represented as mean \pm SEM from seven independent experiments performed in triplicate, and statistical analysis was performed through a paired t test ($*P < 0.05$). (C) Increased lysosomal content during SMC differentiation from hADSCs. The content of intracellular organelles including the mitochondria, ER, and lysosome was measured through flow cytometry by using the fluorescent probes MitoTracker Green, ER Tracker Green, and LysoTracker Green, respectively. Data were represented as mean \pm SEM from at least three independent experiments with triplicate.

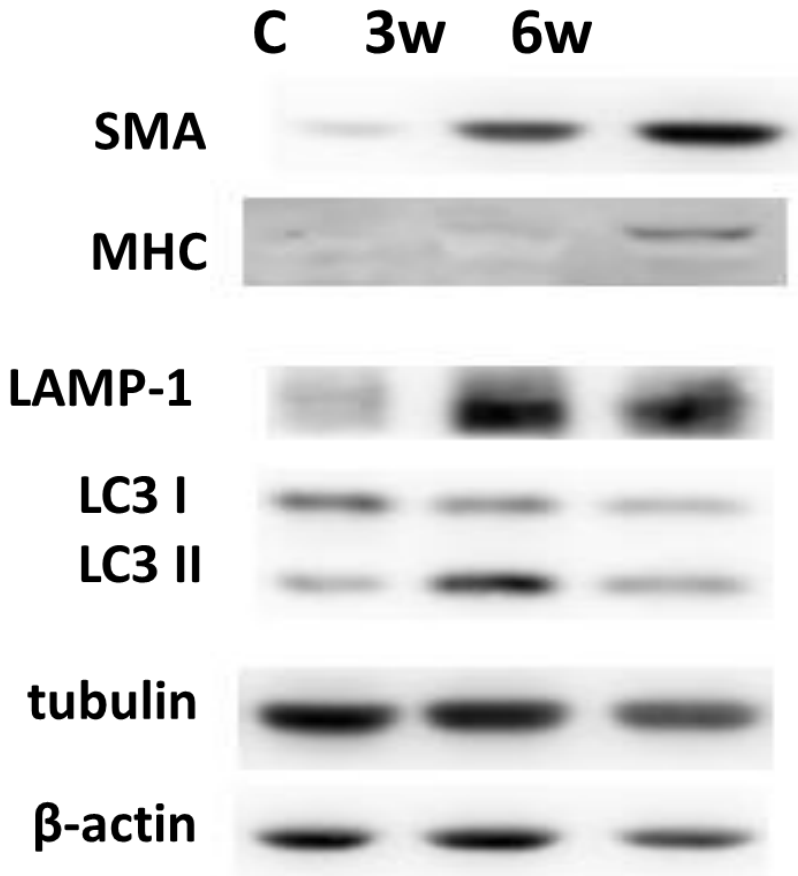


Figure 6. Increased lysosome membrane protein and LC3-II during SMC differentiation from hADSCs. Increased autophagy during SMC differentiation from hADSCs. During SMC differentiation, the protein level of LAMP-1 increased, and the conversion from LC3-I to LC3-II was upregulated. The results were confirmed by at least three independent experiments.

Table 1. Primers used in real-time PCR

Gene	Primers (5'-3')	Product size (bp)
ACTA2 (α -SMA)	Forward - GTGTTGCCCTGAAGAGCAT	109
	Reverse - GCTGGACATTGAAAGTCTCA	
TAGLN (SM22 α)	Forward - GGCAGCTTGGCAGTGACC	101
	Reverse - TGGCTCTCTGTGAATTCCCTCT	
CNN1 (calponin)	Forward- CAACCACCACGCACACA ACTAC	97
	Reverse - GGTCCAGCCAAGAGCAGCAG	
CALD1 (caldesmon)	Forward - CTGGCTTGAAGGTAGGGGTTT	82
	Reverse - TTGGGAGCAGGTGACTTGTTT	
(MYH11) MHC	Forward - CAGGAGTTCGCCAACGCTA	67
	Reverse - TCCCGTCCATGAAGCCTTGG	